



## PRE-DESIGN OF VISCOELASTIC DISSIPATING DEVICES TO REDUCE THE TRANSVERSE DISPLACEMENTS OF AN URBAN CABLE-STAYED BRIDGE

Sonia Ruiz<sup>1</sup>, J. Antonio López-Meza<sup>2</sup>, Francisco L. Silva<sup>3</sup> and Luis Esteva<sup>4</sup>

### ABSTRACT

A solution is presented to reduce the transverse displacements of an urban cable-stayed bridge using viscoelastic energy dissipating devices. A displacement-based dynamic modal method is proposed oriented to design the dampers. The algorithm uses an equivalent single-degree-of-freedom system and uniform hazard pseudo-displacement response spectra. The design method is applied in an illustrative example.

### Description of the problem

An urban cable-stayed bridge is analyzed. It is a steel bridge geometrically similar to one that will probably be constructed in the city of Guadalajara, Jalisco, Mexico, but in this study it is supposed to be located in another city, with a mean annual temperature of 20°C (the minimum and maximum temperatures oscillate between 15°C and 25°C).

The study is focused exclusively on explore possible ways to control, by means of viscoelastic dissipating devices, the bridge transverse displacements caused by the action of the unbalanced live load plus the seismic action. The unbalanced live load is caused by the weight of vehicles acting only on one side of the roadway (for example when traffic is occurring only in one direction). The total live load on the roadway is equal to 1471.25 ton, the unbalanced load (acting on of the roadway) is 735.6 ton, and the total dead load is equal to 4338.3 ton.

The bridge structure includes three segments: a central one (which is cable-stayed) and two at the ends (see figure 1). The central section is 155m long, and is supported by two pairs of steel pylons jointed at their top. The pylons are 40m height and the lengths of the cables range between 27 and 40m. Each pylon is formed by three A-50 steel plates. Only the central segment of the bridge is analyzed here (see figure 1), taking it as independent of the two end segments. A torpedo with circular section run along the longitudinal axis of the deck (see figure 7), and two torpedos run along both sides of the deck.

<sup>1</sup> Professor, Instituto de Ingeniería, Universidad Nacional Autónoma de México, Coyoacan, Z.C. 04510, Mexico, D.F. [sruizg@iingen.unam.mx](mailto:sruizg@iingen.unam.mx)

<sup>2</sup> Graduate student, Instituto de Ingeniería, Universidad Nacional Autónoma de México, Coyoacan, Z.C. 04510, Mexico, D.F. [jlopezm@iingen.unam.mx](mailto:jlopezm@iingen.unam.mx)

<sup>3</sup> Researcher, The Mexican Petroleum Institute, Eje Central Lázaro Cárdenas 152, Z.C. 07730, Mexico, D.F. [flsilva@imp.mx](mailto:flsilva@imp.mx)

<sup>4</sup> Professor Emeritus, Instituto de Ingeniería, Universidad Nacional Autónoma de México, Coyoacan, Z.C. 04510, Mexico, D.F. [lestevam@iingen.unam.mx](mailto:lestevam@iingen.unam.mx)

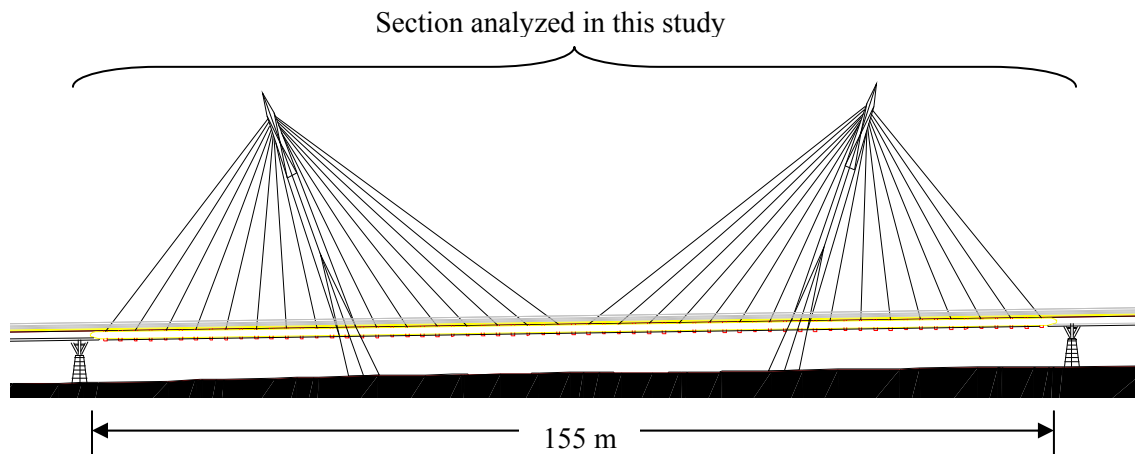


Figure 1. Longitudinal view of the bridge

The 155m central segment of the bridge was modeled mathematically (Zamorano, 2009) in the computer program SAP2000 v.14, as shown in figure 2. In the analysis it was considered the geometric nonlinearity of the cables. The first five natural periods of vibration of the central segment of the bridge are equal to 6.47, 4.19, 2.86, 2.16 and 1.08s.

Figure 3 shows the the fundamental mode configuration, assuming that the central bridge segment does not have any lateral restriction, except that provided by the cables.

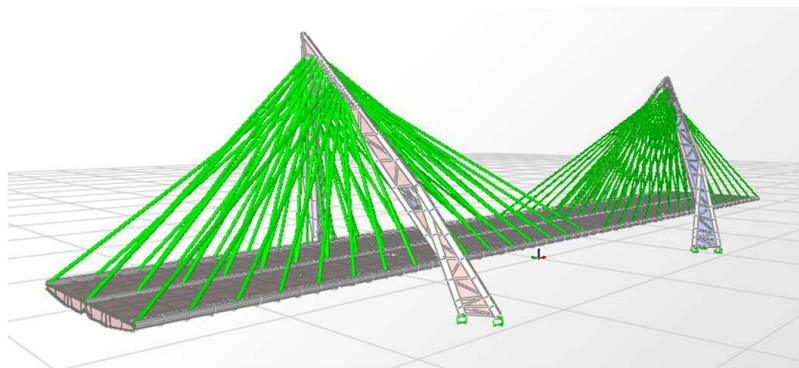


Figure 2. Isometric view of the mathematical model

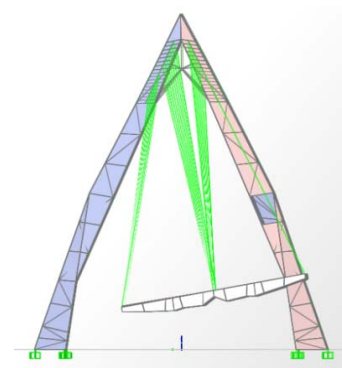


Figure 3. Fundamental mode

### Uniform hazard spectra (UHS)

The seismic hazard curves at the site (corresponding to 5% of critical damping) are supposed to be known. From them, the uniform hazard pseudo-acceleration spectrum (UHS) associated with a 500 years return interval was constructed, and the UHS for different values of critical damping were built using the expression proposed by Esteva (1976). The pseudo-acceleration and displacement UHS for 5, 10, 15, 20, 25, 30 and 35% of critical damping are shown in figures 4a and b.

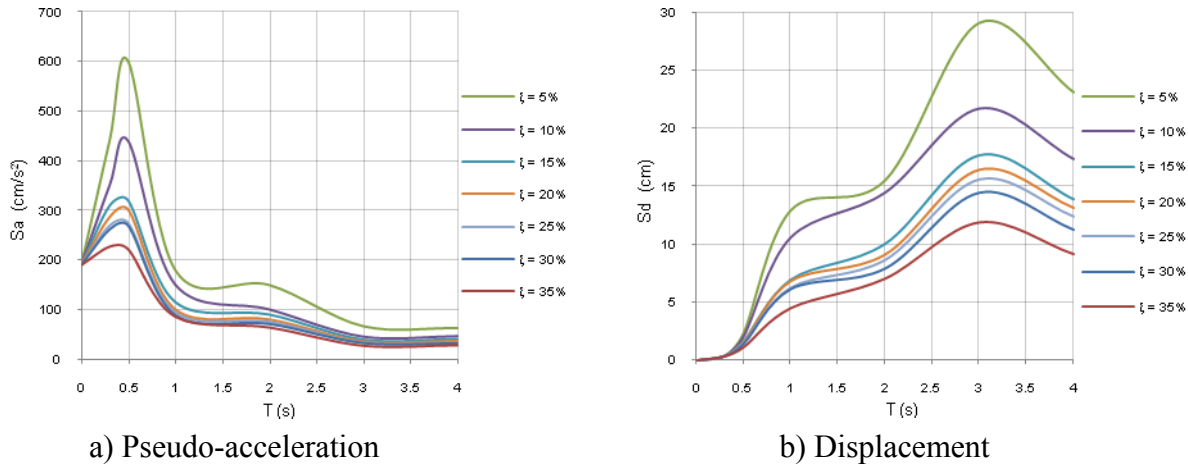
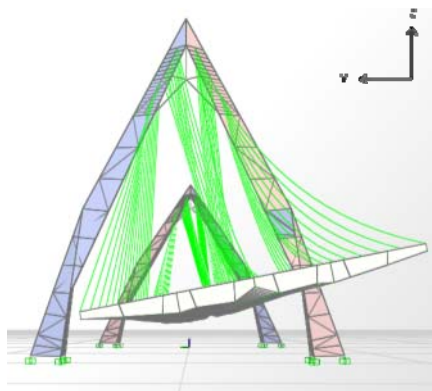


Figure 4. Uniform hazard spectra (UHS)

### Static analysis of the bridge under gravity loads

The central segment of the bridge (called the bridge, in what follows) was analyzed under the action of different distributions of static live loads. The critical load distribution corresponded to the case of the unbalanced live load (traffic only in one direction, while the other side of the deck remains unloaded), here we called it  $LL_{unbalanced}$ . The displacements of the deck at the center of the span under this critical load distribution are presented in figure 5.



$$\Delta_{X_{max}} = 0.0004 \text{ m (longitudinal)}$$

$$\Delta_{Y_{max}} = -2.79 \text{ m (transverse)}$$

$$\Delta_{Z_{max}} = 0.87 \text{ m (vertical)}$$

where:

$\Delta_{X_{max}}$  is the maximum displacement in X direction

$\Delta_{Y_{max}}$  is the maximum displacement in Y direction

$\Delta_{Z_{max}}$  is the maximum displacement in Z direction

Figure 5. Shape of the bridge under unbalanced live load

From the displacements shown in figure 5, it is clear that it is necessary to reduce the transverse displacements of the deck.

### Dynamic analysis under the combination of seismic motions plus unbalanced live load

Next, the bridge was analyzed with the worst combination of live load plus seismic action. It corresponded to the following:  $0.8 LL_{unbalanced} + 0.3 S_x + 1.0 S_y$ ; where  $S_x$  = motion in X direction,  $S_y$  = motion in Y direction. The unbalanced live load was reduced by a factor of 0.80

because there is a low probability that the seismic motion occurs at the same time that the maximum unbalanced live load is acting. Using this load condition, the following displacements are obtained:  $\Delta_{X_{max}} = 0.043$ ;  $\Delta_{Y_{max}} = -2.87$  m;  $\Delta_{Z_{max}} = -0.94$ m.

**Solution for controlling the transverse displacements, using passive seismic energy dissipating devices**

An approach is presented to reduce the transverse displacements trough the use of viscoelastic energy dissipating devices located at the base of the bridge (see figures 6 and 7). In addition, it is necessary to place a set of springs located at both ends of the central segment of the bridge (see figure 8).

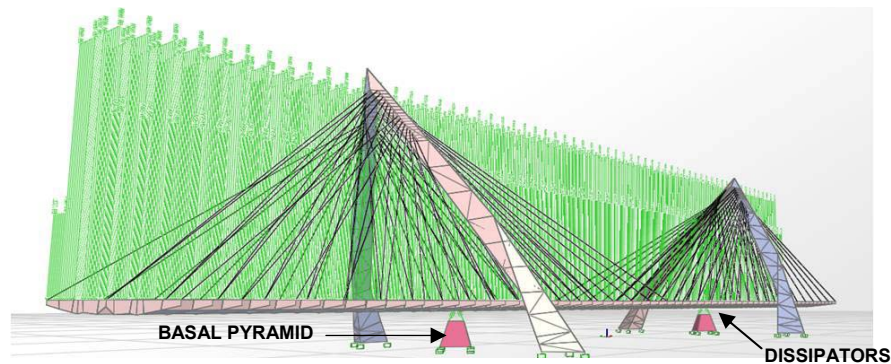


Figure 6. Isometric view of the bridge and dissipating devices under the deck

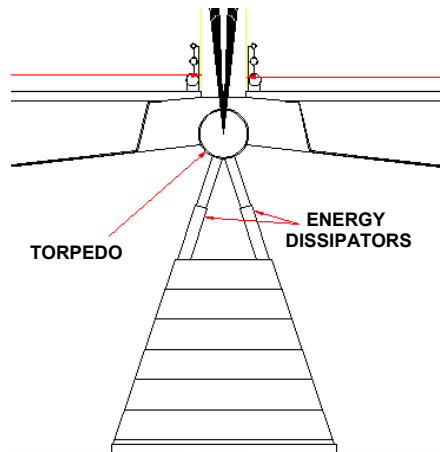


Figure 7. Pyramid and dissipating devices

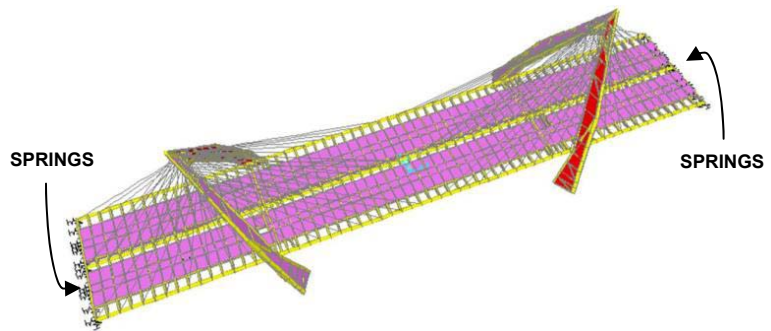


Figure 8. Location of springs

**Design of viscoelastic seismic energy dissipating devices**

An algorithm is proposed in the following for the analysis and design of the dissipating devices. The method includes two steps (A and B). The first one (A) is intended to reducing the effect of the unbalanced live load (assumed here as static load). The second step (B) consists in a modal dynamic analysis that takes into account the effect of the unbalanced live loads plus the seismic action.

**Part A) Lateral stiffness necessary to limit the transverse displacements of the bridge due to the unbalanced live load**

For the purpose of preliminary evaluation of the seismic response of the bridge, it is represented by a single-degree-of-freedom system consisting in a vertical bending element fixed at its base.

In order to calculate the stiffness of the equivalent system, a set of horizontal loads ( $P_i$ ) acting in the transverse sense (parallel to the Y axis) is applied to the bridge, as shown in figure 9. As a consequence, we obtain the horizontal displacements  $\delta_i$  along the Y axis.

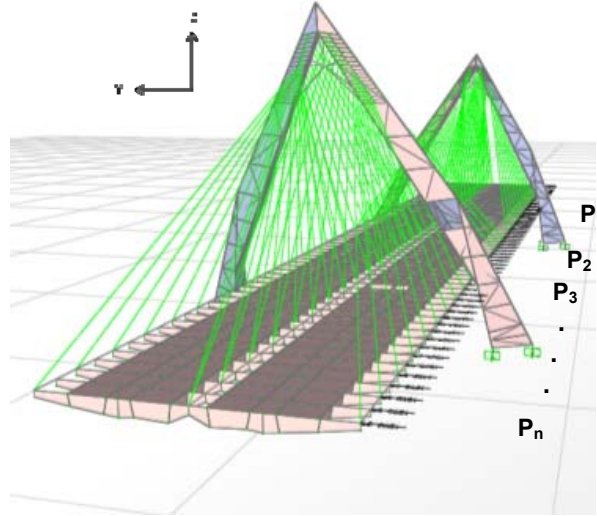


Figure 9. Horizontal loads applied to the structure

The equivalent transverse displacement of the SDOF is calculated by means of the following expression (Calvi and Kingsley, 1995):  $\delta_e = \sum_1^n \delta_i^2 / \sum \delta_i$ . Using this, the equivalent stiffness of the SDOF results equal to  $K_e = \sum P_i / \delta_e$ . This value of the equivalent lateral stiffness of the system ( $K_e$ ) is used to obtain the force ( $F_{LLunbalanced}$ ) that gives place to the transverse displacement ( $\delta_{LLunbalanced}$ ) that takes place in the SDOF under the action of the unbalanced static load  $F_{LLunbalanced} = K_e \cdot \delta_{LLunbalanced}$ .

A target value of the transverse displacement ( $\delta_{obj}$ ) is next selected. The lateral stiffness ( $K_L$ ) needed to get that displacement is:

$$K_L = \frac{F_{LLunbalanced}}{\delta_{obj}} \quad (1)$$

The stiffness  $K_L$  will be taken by the viscoelastic dampers located at the base of the bridge and by the horizontal springs that will be placed at both ends of its central section.

## B) Iterative modal analysis

The following paragraphs describe the steps of an iterative modal dynamic method that considers the effects of the seismic load plus the unbalanced live load.

**Step 1)** A tentative value is proposed for the percentage of the lateral stiffness that will be taken by the viscoelastic dampers ( $K_{dT}$ ). The remaining percentage of the lateral stiffness will be taken by the horizontal springs located at the ends of the bridge ( $K_{rT}$ ), and by the deck-cable system ( $K_e$ ). This is expressed as follows:

$$K_L = K_{dT} + K_{rT} + K_e \quad (2)$$

$$K_{dT} = \lambda \cdot (K_L - K_e) \quad (3)$$

where:  $K_L$  is the stiffness calculated with equation 1;  $K_{dT}$  is the stiffness provided by the viscoelastic devices;  $K_{rT}$  is the stiffness provided by the horizontal springs that will be placed at the ends of the bridge;  $K_e$  is the stiffness provided by the deck-cable system, and  $\lambda$  represents a percentage value,  $0 \leq \lambda \leq 1$ .

**Step 2)** Next, a period of vibration ( $T_s$ ) corresponding to the fundamental mode of the bridge + dissipators + springs is proposed.

**Step 3)** Uniform-hazard displacement response spectra are established, corresponding to the time interval selected for the limit state of interest. Using the target displacement ( $\delta_{obj}$ ) and the period  $T_s$  proposed according to Step 2, the effective value of the fraction of critical damping  $\xi_t$  that satisfies the pair of values ( $T_s, \delta_{obj}$ ) is obtained.

**Step 4)** Next, it is verified that the fraction of critical damping  $\xi_e$  corresponding to the viscoelastic dissipators satisfies equation 4, where  $\xi_e$  is equal to the difference between the effective damping and the inherent damping of the structure  $\xi_e = \xi_t - \xi_i$ :

$$\xi_e = \frac{G''}{2G'} \quad (4)$$

Here,  $G'$  and  $G''$  are the storage and loss shear modules of the viscoelastic material, respectively.

In the case that the  $\xi_e$  value obtained from the UHS differs significantly from that obtained with equation 4, it will be necessary to propose a new value of  $\lambda$  (see equation 3) and a new period of vibration of the system ( $T_s$ ); otherwise, the process continues to the next step.

**Step 5)** The value of the damping coefficient ( $C_{dT}$ ) is calculated with the following equation:

$$C_{dT} = \frac{2\xi_e K_{dT}}{\omega_s} \quad (5)$$

where  $\omega_s$  it is the natural frequency that corresponds to the vibration period proposed:  $\omega_s = 2\pi / T_s$ .

**Step 6)** Once the  $K_{dT}$  and  $C_{dT}$  values are known, they are distributed among the number of devices that will be placed in the system.

**Step 7)** Next the bridge + dissipators + springs system is analyzed, in order to verify that the target displacement is reached in the mathematical model.

**Step 8)** Finally, it must be checked that the deformations of the viscoelastic devices (in local coordinates) are smaller than the allowable ones (obtained from laboratory tests).

The iterative process is maintained until convergence is achieved.

In the section that follows the methodology described is applied to the cable-stayed bridge described previously. Only the near-collapse limit state is considered; however, the methodology can be applied to other limit states. Also, only the case corresponding to an environmental average temperature equal to 20°C, which corresponds to the average temperature at the hypothetical location of the bridge, is assumed; this is taken to imply that the temperatures at the site during spring and winter are not very different.

### Application of the proposed methodology

#### *A) Stiffness required to attain a specified target displacement ( $\delta_{obj}$ )*

In this example, a horizontal load  $\sum P_i = 63$  Ton is applied along the longitudinal axis of the bridge. The equivalent stiffness results equal to  $K_e = 628.5$  Ton/m, and the displacement corresponding to the unbalanced load  $\delta_{unbalanced} = 2.23$ m. Then, a target displacement equal to  $\delta_{obj} = 0.07$  m is selected. The necessary lateral stiffness  $K_L$  resulted as follows (see equation 2):

$$K_L = \frac{1.401 \times 10^3}{0.07} = 2.002 \times 10^3 \text{ Ton/m}$$

#### *B) Iterative modal analysis*

Each of the steps proposed in the algorithm were followed in the example; however, due



to space limitations, only the final iteration results are presented.

**Step 1)** The stiffness ( $K_e$ ), provided by the deck-cable system, is subtracted from the stiffness  $K_L$ . The remaining stiffness value is distributed between the viscoelastic devices and the horizontal springs (equation 3):  $K_{dT} + K_{rT} = 1.939 \times 10^4$  Ton/m.

After a few iterations,  $\lambda$  resulted equal to 0.65 (equation 4); that is,  $K_{dT} = (0.65)(1.939 \times 10^4$  Ton/m) =  $1.260 \times 10^4$  Ton/m. Therefore, the lateral stiffness provided by the horizontal springs should be  $K_{rT} = (0.35)(1.939 \times 10^4) = 6.788 \times 10^3$  Ton/m.

**Step 2)** The value  $T_s = 2.12$  s is proposed for the fundamental natural period of vibration of the combined system; thus, the cyclic frequency is  $f_s = 1/T_s = 0.472$  Hz.

**Step 3)** For the proposed values of the fundamental period of vibration ( $T_s = 2.12$ s) and target displacement  $\delta_{obj} = 0.07$ m) the effective value of critical damping is equal to  $\xi_i = 35\%$ , according to the displacement uniform hazard spectra shown in figure 4b. (This result is verified in the next steps.)

**Step 4)** The percentage of critical damping attributed to the viscoelastic system is  $\zeta_e = 33$  percent, and that corresponding to the inherent damping of the original system is assumed to be  $\xi_i = 2$  percent; therefore, the effective critical damping of the system is 35 percent.

In order to verify the level of critical damping provided by the viscoelastic devices, use is made of equation 5, where the values of  $G'$  and  $G''$  depend on the type of viscoelastic material used. Here, the experimental results presented by Zimmer (2000) are used. Figures 10 a and b show those results, which correspond to an environmental temperature  $T = 20^\circ\text{C}$ .

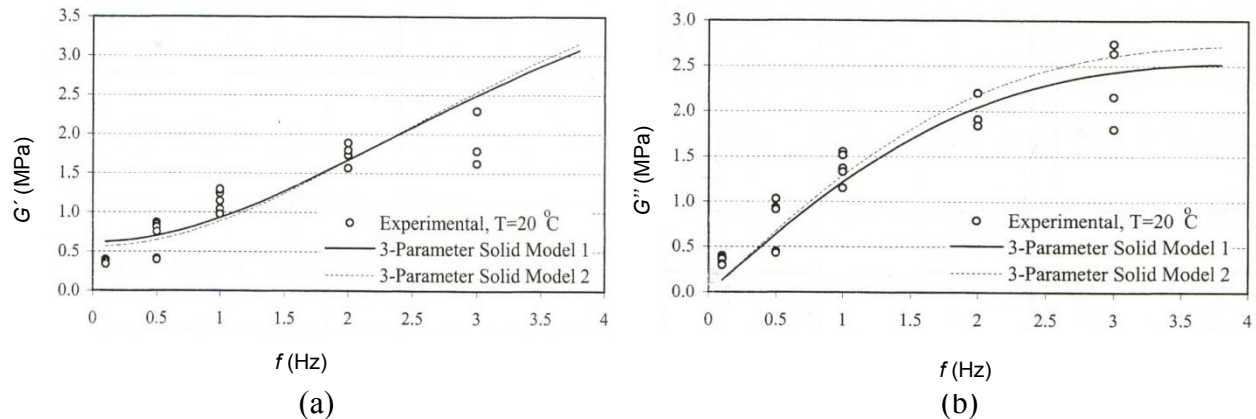


Figure 10. Values of the storage ( $G'$ ) and loss shear ( $G''$ ) modules, as functions of the frequency.  $T = 20^\circ\text{C}$  (Zimmer, 2000).



From figures 10a and b, the following values are obtained:  $G' = 0.81 \text{ MPa} = 82.597 \text{ Ton/m}^2$ ;  $G'' = 0.535 \text{ MPa} = 54.55 \text{ Ton/m}^2$ . Inserting these values in equation 5 leads to:  $\xi_e = 54.55 / (2 \times 82.597) = 0.33$ . This is the same value obtained in Step 4. Therefore, this confirms that the effective critical damping of the system, obtained as the sum of the contributions of the viscoelastic dampers and of the inherent damping of the system, is equal to 35%. This value corresponds to that shown in the UHS (figure 4b); thus, it is concluded that the assumed values of both the fundamental period and the factor  $\lambda$  are correct

**Step 5)** Next, the damping coefficient  $C_{dT}$  is calculated (equation 6):  
 $C_{dT} = 2 \cdot \xi_e \cdot K_{dT} / \omega_s = 2.807 \times 10^3 \text{ Ton-s/m}$ .

**Step 6)** Twelve dissipating devices are introduced in two basal pyramids, similar to that shown in Figure 11. The lateral stiffness  $K_{dT}$  should be distributed in that number of devices.

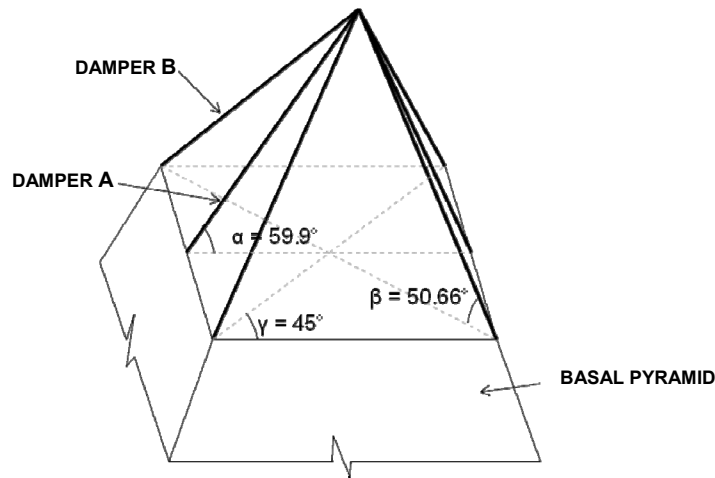


Figure 11. Isometric view of the basal pyramid, showing the locations of six dampers

Figure 12 and Table 1 summarize the properties of the viscoelastic dampers resulting from the design process.

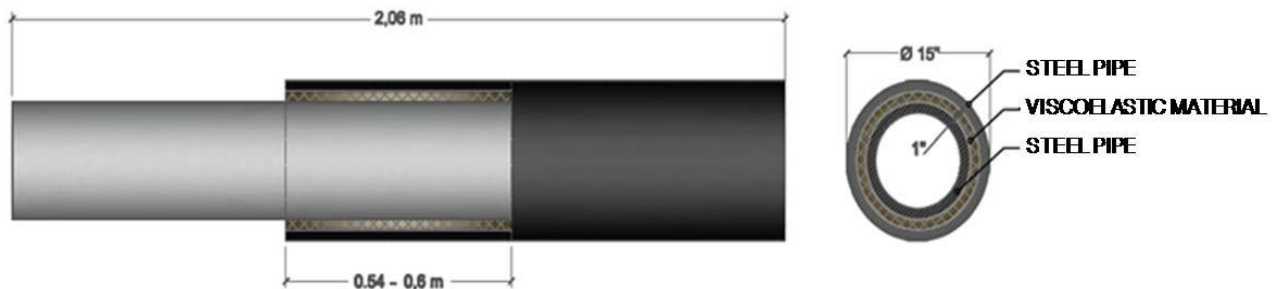


Figure 12. Viscoelastic damper (type A)

Table 1. Properties of the viscoelastic dampers

<b>Damper</b>	<b>Lenght (m)</b>	<b>Area (m<sup>2</sup>)</b>	<b>Thickness (m)</b>	<b>K<sub>d</sub> (Ton/m)</b>	<b>C<sub>d</sub> (Ton-s/m)</b>
<b>A</b>	0.54	0.644	0.0254	2.094 x 10 <sup>3</sup>	466.67
<b>B</b>	0.60	0.721	0.0254	2.343 x 10 <sup>3</sup>	522.46

### *Design of horizontal springs*

In order to design the horizontal springs to be placed at the ends of the central segment of the bridge, the total stiffness determined in the previous paragraphs is divided between the number of devices. Here, 26 devices are introduced:

$$K_{dRi} = \frac{K_{dR}}{26} = \frac{6.788 \times 10^3}{26} = 261.08 \text{ Ton/m}$$

**Step 7)** A modal analysis using the computer program SAP2000 v.14 was carried out. The seismic spectrum used is that of figure 4a. The maximum displacement at the center of the span was equal to 0.065 m (notice that the target value was  $\delta_{obj} = 0.07\text{m}$ ), and the maximum displacement at the ends was 0.047 m.

**Step 8)** Finally, it was verified that the strains developed by the viscoelastic material remained below the allowable limit.

### **Concluding remarks**

The solution presented here is theoretical and has not been implemented in the field. The resulting viscoelastic devices are larger than those found by the authors in the literature. An uncertainty remains about the possible behavior of devices larger than those for which experimental cyclic-load test results are available.

### **Acknowledgements**

The present study was carried out with support of the Universidad Nacional Autónoma de México under project DGAPA - PAPIIT IN108708.

### **References**

- Calvi G.M., Kingsley G.R., 1995, Displacement-based seismic design of multi-degree-of-freedom bridge structures, *Journal of Earthquake Engineering and Structural Dynamics* (24), 1247-1266.
- Esteva (1976), *Seismicity*, Book Chapter 6: Seismic Risk and Engineering Decisions. Edited by C. Lomnitz and E. Rosenblueth, Elsevier, 179-224.
- Zamorano, F., 2009, Personal communication.